Articles

Synthesis and Characterization of Iodine-123 Labeled 2β-Carbomethoxy-3β-(4′-((*Z*)-2-iodoethenyl)phenyl)nortropane. A Ligand for in Vivo Imaging of Serotonin Transporters by Single-Photon-Emission Tomography

Mark M. Goodman,*[,†,‡] Ping Chen,[†] Christophe Plisson,[†] Laurent Martarello,[†] James Galt,[†] John R. Votaw,[†] Clinton D. Kilts,[‡] Gene Malveaux,[†] Vernon M. Camp,[†] Bing Shi,[†] Timothy D. Ely,[‡] Leonard Howell,[§] Jon McConathy,[†,‡] and Charles B. Nemeroff[‡]

Department of Radiology, Department of Psychiatry and Behavior Sciences, and Yerkes Regional Primate Center, Emory University, Atlanta, Georgia 30320

Received January 1, 2001

2β-Carbomethoxy-3β-(4′-((*Z*)-2-iodoethenyl)phenyl)nortropane (ZIENT) (**6**) and 2β-carbomethoxy-3β-(4′-((*E*)-2-iodoethenyl)phenyl)nortropane (EIENT) (**10**) were prepared and evaluated in vitro and in vivo for serotonin transporter (SERT) selectivity and specificity. High specific activity [^{123}I]ZIENT and [^{123}I]EIENT were synthesized in 45% (n = 5) and 42% (n = 4) radiochemical yield (decay-corrected to end of bombardment (EOB)), respectively, by preparation of the precursor carbomethoxy-3β-(4′-((*Z*)-2-trimethylstannylethenyl)phenyl)nortropane (**7**) and 2β-carbomethoxy-3β-(4′-((*E*)-2-tributylstannylethenyl)phenyl)nortropane (**9**), respectively, followed by treatment with no carrier-added sodium [^{123}I]iodide and hydrogen peroxide in ethanolic HCl. Competition binding in cells stably expressing the transfected human SERT, dopamine transporter (DAT), and norepinephrine transporter (NET) using [^{3}H]citalopram, [^{3}H]WIN 35,428, and [^{3}H]nisoxetine, respectively, demonstrated the following order of SERT affinity (K_i in nM): ZIENT (0.05) > nor-CIT (0.12) ≫ EIENT (1.15) > fluvoxamine (1.46). The affinity of ZIENT and EIENT for DAT was 69 and 1.6-fold lower, respectively, than for SERT. In vivo biodistribution and blocking studies were performed in male rats and demonstrated that the brain uptake of [^{123}I]ZIENT was selective and specific for SERT-rich regions (hypothalamus, striatum, pons, and prefrontal cortex). SPECT brain imaging studies in monkeys demonstrated high [^{123}I]ZIENT uptake in the diencephalon, which resulted in diencephalon-to-cerebellum ratios of 2.12 at 190 min. [^{123}I]ZIENT uptake in the diencephalon achieved transient equilibrium at 157 min. In a displacement experiment of [^{123}I]ZIENT in a cynomolgus monkey, radioactivity was reduced by 39% in the diencephalon at 101 min following injection of citalopram. The high specific activity one-step radiolabeling preparation and high selectivity of [^{123}I]ZIENT for SERT support its candidacy as a radioligand for mapping brain SERT sites.

Introduction

The serotonin transporter (SERT) is a protein that resides on the presynaptic membranes of serotonin synthesizing neurons. The SERT is a sodium/potassium adenosine triphosphate dependent carrier and regulates serotonergic transmission by removing serotonin from the synapse back into the cell cytosol for subsequent storage into secretory vesicles. Serotonergic neurons originate primarily from neuronal cell bodies of the medial and dorsal raphe in the brainstem and innervate discrete areas that include the hypothalamus, thalamus, striatum, and cerebral cortex. Considerable evidence has convincingly implicated SERT in the pathophysiology of major depression.[1] These findings include (a) decreased numbers of SERT binding sites in postmortem brain tissue of depressed patients and suicide victims,[2−4] (b) reduced concentrations of serotonin transporters on peripheral platelets of depressed patients,[5] and (c) clinically efficacious antidepressant activity associated with inhibitors of serotonin reuptake. Alterations in SERT density have been implicated not only in depression but also in Alzheimer's disease,[6] Parkinson's disease,[7,8] and the neurotoxic effects of the illicit drug 3,4-methylenedioxyamphetamine (Ecstasy).[9] Moreover, binding studies with [^{3}H]-(−)-cocaine have demonstrated that cocaine binds to SERT.[10] Thus, cocaine's inhibition of serotonin reuptake and the resulting increase of serotonin in the synapse may contribute to the mechanism that supports the link between SERT and cocaine's reinforcing properties. Although a large and consistent body of data supporting the link between the SERT and depression have been obtained, this

* To whom correspondence should be addressed. Address: Department of Radiology, Emory University, 1364 Clifton Road, NE, Atlanta, GA 30322. Phone: (404) 727-9366. Fax: (404) 727-3488. E-mail: mgoodma@emory.edu.
† Department of Radiology.
‡ Department of Psychiatry and Behavior Sciences.
§ Yerkes Regional Primate Center.

10.1021/jm0100180 CCC: $25.00
Published on Web 02/15/2003

supporting evidence is largely indirect because it is derived almost exclusively from the study of postmortem tissue and peripheral cells models. The development of radioligands to characterize the in vivo distribution, density, and occupancy of the SERT by emission tomography techniques would present unique opportunities to define the function and pharmacology of the SERT in the living human brain and perhaps aid both in diagnosing depression and in monitoring response to therapy.

Numerous efforts have been made to develop SERT imaging agents labeled with the γ-emitting radionuclide iodine-123 to study the roles of this neuroregulatory site using single-photon-emission computed tomography (SPECT). Iodine-123 is an attractive radionuclide for SPECT imaging because iodine-123 emits abundant (85%) 159 keV photons, which is suitable for clinical γ-cameras, and has a 13.3 h half-life, which is ideal for imaging radioligands requiring a longer period of time to reach a binding equilibrium. Dynamic imaging studies of the SERT in nonhuman primates with iodine-containing radioligands by SPECT have been reported. A series of *R*- and *S*-tomoxetine derivatives, a close structural analogue of fluoxetine, in which iodine was introduced into the ortho, meta, and para positions of the phenoxy ring showed high in vitro affinity and selectivity for SERT.[11] Imaging studies in nonhuman primates with the highest affinity and selective derivative, (*R*)-(−)-*N*-methyl-3-(4-iodo-2-methylphenoxy)-3-phenylpropanamine, were performed.[12] Unfortunately, the in vivo affinity and selectivity for the SERT of this radioiodinated ligand did not reflect its in vitro properties and resulted in poor-quality images of brain regions rich in SERT. The nontricyclic antidepressant 6-nitroquipazine is a potent and selective SERT inhibitor.[13,14] In vivo studies in mice with [^{3}H]-6-nitroquipazine demonstrated rapid and high brain uptake with specific uptake and retention in brain regions rich in SERT.[15] A radioiodine-labeled nitroquipazine derivative has been reported that exhibited selective binding to SERT. Serial SPECT imaging in nonhuman primates demonstrated that [^{123}I]-5-iodo-6-nitroquipazine accumulated in SERT-rich brainstem. However, this radioligand was cleared slowly from brain regions of low SERT density, requiring measurement at 5−8 h after injection.[16,17] More recently, iodine-123 labeled ADAM, 2-([2-([dimethylamino)methyl]phenyl]thio)(5-iodophenylamine),[18,19] demonstrated high in vitro binding and selectivity to the SERT with low affinity to DAT and NET. A SPECT imaging study in baboons demonstrated [^{123}I]ADAM uptake in the midbrain with midbrain-to-cerebellum ratios of 2.1 accompanied by a transient equilibrium established at 138 min after injection[20] and supported its candidacy for imaging SERT sites by SPECT.

Competitive binding studies demonstrated that a series of nor-3β-4′-substituted phenylcocaine analogues have an order of magnitude higher affinity for the SERT than their corresponding *N*-methyl analogues.[21] The highest affinity analogue 2β-methoxycarbonyl-3β-(4′-iodophenyl)nortropane (nor-CIT) had a much higher affinity for the SERT, $IC_{50} = 0.36$ nM, when compared to 2β-methoxycarbonyl-3β-(4′-iodophenyl)tropane (CIT), $IC_{50} = 4.2$ nM. Radioiodinated CIT[22,23] and nor-CIT[24] have been employed as radiotracers for in vivo SPECT imaging of SERT sites. Because CIT is a nonselective SERT ligand with high affinity for the DAT as well as for the SERT, quantitative imaging of the SERT in humans with [^{123}I]RTI-55 (CIT) was possible only when the DAT sites were preblocked.[23] Iodine-123 labeled nor-CIT[24] has been evaluated in rats and showed high uptake in brain regions of high SERT density, such as the hypothalamus where the uptake of radioactivity was significantly reduced in animals preblocked with fluvoxamine, a selective SERT inhibitor. However, nor-CIT also has a high binding affinity for the DAT[21] ($IC_{50} = 0.36$ nM) and therefore suffers from the same shortcomings in selectivity as CIT. Thus, nor-CIT is not an ideal radioligand for measuring SERT density by SPECT.

In attempts to develop a 2β-propanoyl-3β-arylnortropane possessing high binding affinity to the SERT and low binding affinity to DAT and NET, Davies and co-workers synthesized two analogues containing ethenyl and methylethenyl substituents at the 4′-position of the 3β-phenyl ring.[25] The resulting compounds 3β-(4′-(1-methylethenyl)phenyl)-2β-propanoyl-8-azabicyclo[3.2.1]-octane and 3β-(4′-(ethenyl)phenyl)-2β-propanoyl-8-azabicyclo[3.2.1]octane had high affinity for SERT ($IC_{50} = 0.16$ nM and $IC_{50} = 0.32$ nM, respectively vs [^{3}H]-paroxetine). However, only the 1-methylethenyl analogue demonstrated high selectivity for SERT vs DAT and NET. Carroll and co-workers synthesized a series of analogues containing alkenyl substituents at the 4′-position of the 3β-phenyl ring in 2β-methoxycarbonyl-3β-arylnortropane.[26] These studies revealed that introduction of propenyl groups afforded analogues with high affinity and selectivity for SERT. 2β-Carbomethoxy-3β-(4′-*cis*-propenylphenyl)nortropane (nor-β-CCPPT) and 2β-carbomethoxy-3β-(4′-*trans*-propenylphenyl)nortropane (nor-β-CTPPT) were found to be two of the highest affinity alkenyl analogues. Nor-β-CCPPT showed nanomolar affinity for the SERT ($IC_{50} = 1.15$ nM vs [^{3}H]-paroxetine) and was found to be 28 times more selective for the SERT than the DAT ($IC_{50} = 32$ nM vs [^{3}H]WIN 35,428). Nor-β-CTPPT possessed high affinity for the SERT ($IC_{50} = 1.3$ nM vs [^{3}H]paroxetine) and was found to be 22 times more selective for the SERT than for the DAT ($IC_{50} = 28$ nM vs [^{3}H]WIN 35,428). These results suggested that the 3β-4′-vinyl substituent could allow the introduction of an trialkyltin substituent, enabling incorporation of iodine-123 as either a *Z*-iodovinyl or an *E*-iodovinyl group, and potentially lead to a high-affinity and selective radioligand for in vivo SERT imaging. We report here the synthesis, in vitro characterization, radiosynthesis, ex vivo regional brain distribution in rats, and SPECT imaging in a nonhuman primate of 2β-carbomethoxy-3β-(4′-((*Z*)-2-iodoethenyl)phenyl)nortropane (ZIENT) and 2β-carbomethoxy-3β-(4′-((*E*)-2-iodoethenyl)phenyl)nortropane (EIENT) as potential SPECT SERT imaging agents.

Chemistry

The synthetic route chosen for the preparation of the 2β-carbomethoxy-3β-(4′-(2-iodoethenyl)phenyl)nortropanes involved introduction of the iodine at the 2-position of the 3β-4′-vinyl substituent by both a Wittig reaction and iododestannylation of a trialkyltin precursor. The (*Z*)-2-iodoethenyl isomer, ′ZIENT (**6**), was prepared in a five-step sequence of reactions delineated

Scheme 1[a]

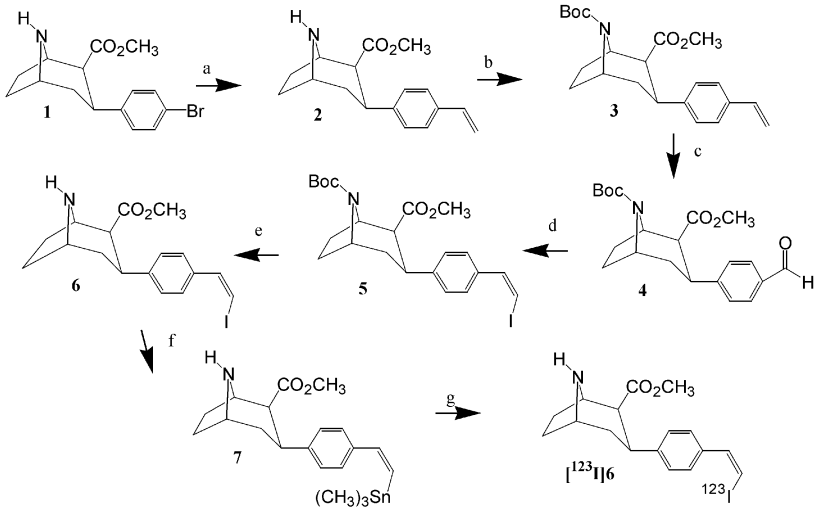

[a] Reagents: (a) $Bu_3SnCH{=}CH_2/Pd(Ph_3P)_4$; (b) $(Boc)_2O$; (c) OsO_4, $NaIO_4$; (d) $(Ph_3P)CH_2I_2$, $((CH_3)_3Si)_2NNa$; (e)TFA; (f) $Me_3SnSnMe_3$, $Pd(Ph_3P)_4$; (g) Na[^{123}I]I, H_2O_2, HCl.

Scheme 2[a]

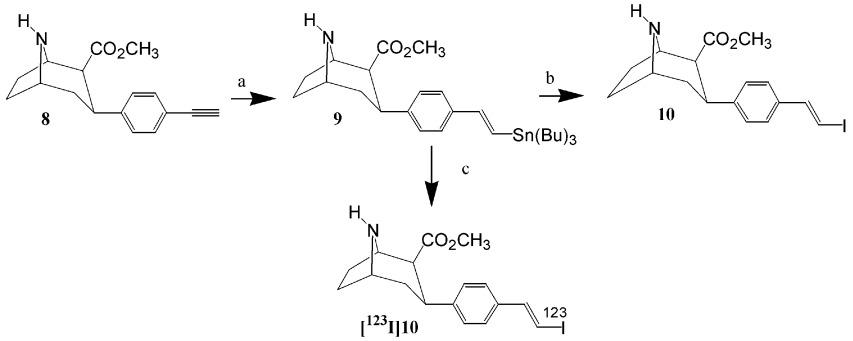

[a] Reagents: (a) Bu_3SnH/AIBN; (b) I_2; (c) Na[^{123}I]I, H_2O_2.

in Scheme 1. In this synthetic approach, 2β-carbomethoxy-3β-(4′-bromophenyl)nortropane (**1**) was treated with tributylvinyltin using Stille reaction conditions to form 2β-carbomethoxy-3β-(4′-ethenylphenyl)nortropane (**2**).[26] The vinylnortropane derivative **2** was converted to *N*-Boc-2β-carbomethoxy-3β-(4′-ethenylphenyl)nortropane (**3**) by treatment with di-*tert*-butyl dicarbonate. Treatment of **3** with osmium tetroxide gave *N*-Boc-2β-carbomethoxy-3β-(4′-formylphenyl)nortropane (**4**). The pivotal step in the synthesis of ZIENT involved introduction of iodine onto the 4′-ethenylphenyl group in the *Z*-configuration by reaction of the formyl intermediate **4** with triphenylphosphoniumiodomethylene ylid to give *N*-Boc-2β-carbomethoxy-3β-(4′-((*Z*)-2-iodoethenyl)phenyl)-nortropane (**5**) and *N*-Boc-2β-carbomethoxy-3β-(4′-ethenyl)phenyl)nortropane (**3**). Analysis of the mixture by reverse-phase HPLC indicated that **5** and **3** were formed. The mixture of olefins was separated by flash chromatography. Removal of the *N*-Boc group gave ZIENT (**6**). In ^{1}H NMR, the (*Z*)-2-iodoethenylphenyl-nortropane **6** exhibited a doublet centered at δ 6.5 with the expected coupling constant $J = 8.7$ Hz for the cis vinylic proton geminal to the iodine group and a doublet at δ 7.20−7.28 for the proton geminal to the phenyl group.

The route developed for the preparation of EIENT (**10**) involved the use of the previously reported 2β-carbomethoxy-3β-(4′-ethynyl)phenyl)nortropane (**8**)[26] (Scheme 2). The key step in the synthesis involved introduction of iodine into the 4′-ethynylphenyl group in the *E*-configuration by hydrostannylation with tri-*n*-butyltin hydride and AIBN to give a 95:5 mixture of 2β-carbomethoxy-3β-(4′-((*E*)-2-tributylstannylethenyl)-phenyl)nortropane (**9**) and 2β-carbomethoxy-3β-(4′-((*Z*)-2-tributylstannylethenyl)phenyl)nortropane. Iododestannylation of **9** by treatment with I_2 in methylene chloride gave EIENT, **10**. The *E*-configuration was assigned to **10** by ^{1}H NMR spectral analysis. EIENT exhibited a doublet centered at δ 6.77 for the proton geminal to the iodine, with a large coupling constant $J = 14.8$ Hz and a doublet centered at δ 7.38 for the trans vinylic proton geminal to the phenyl group with the same coupling constant $J = 14.8$ Hz.

Radiochemistry

The radioiodinated 2β-carbomethoxy-3β-(4′-((*Z*)-2-[^{123}I]iodoethenyl)phenyl)nortropane (**6**) and 2β-carbomethoxy-3β-(4′-((*E*)-2-[^{123}I]iodoethenyl)phenyl)nortropane (**10**) were prepared by no carrier-added Na^{123}I treatment of their corresponding tin precursors with I^+ generated in situ by H_2O_2/EtOH·HCl oxidation of radioiodide. The preparation of the *Z* isomer, [^{123}I]**6**, involved iododestannylation of the trimethylstannyl precursor 2β-carbomethoxy-3β-(4′-(*Z*)-2-trimethylstannylethenylphenyl)nortropane (**7**). The trimethylstannyl precursor **7** was prepared in 10% yield by treatment of

Table 1. Inhibition Constants (K_i, nM) of Various Ligands for Stably Transfected Monoamine Transporters

	K_i of human monoamine transporter				
ligand	DAT[a]	SERT[b]	NET[c]	DAT/SERT ratio	NET/SERT ratio
CIT	0.48	0.67	1.4	1.4	1.4
ZIENT	3.47	0.05	24	69	474
EIENT	1.88	1.15	32	1.63	19.6
nor-CIT		0.12			
fluvoxamine		1.46			
desipramine			0.49		
reboxetine		60	9		0.15
nisoxetine		30	1.4		0.05

[a] Competitive binding versus [*N*-methyl-^{3}H]-WIN 35428 in murine kidney cells transfected with cDNA for the human dopamine transporter. [b] Competitive binding versus [^{3}H]citalopram in murine kidney cells transfected with cDNA for the human serotonin transporter. [c] Competitive binding versus [^{3}H]nisoxetine in murine kidney cells transfected with cDNA for the human norepinephrine transporter.

6 with hexamethylditin. Attempts to prepare a tributylstannyl precursor in the *Z*-configuration by hydrostannylation with tri-*n*-butyltin hydride in the absence or presence of AIBN resulted only in the formation of trace amounts of the *Z* tributylstannyl product. The *Z*-configuration was assigned to **7** by ^{1}H NMR spectral analysis. The trimethylstannyl precursor **7** exhibited a doublet centered at δ 6.16, with a coupling constant J = 8.8 Hz, for the proton geminal to the iodine and a doublet centered at δ 7.53, with the same coupling constant J = 8.8 Hz, for the cis vinylic proton geminal to the phenyl group. The tin precursors **7** and **9** were purified by semipreparative reverse-phase HPLC purification prior to radiolabeling.

Biological Results

The in vitro affinity of ZIENT and EIENT for the SERT was determined by competition in a SERT radioligand binding assay using [^{3}H]citalopram binding to homogenates of murine kidney cells stably expressing the human SERT (Table 1). The rank order of SERT affinities was ZIENT > nor-CIT > CIT > EIENT > fluvoxamine > nisoxetine > reboxetine. ZIENT had 2.4 and 23 times higher affinity than nor-CIT and EIENT, respectively, for the human transfected SERT. Competition binding site analyses were also used to evaluate the comparative affinity of ZIENT and EIENT for the human DAT and NET labeled by [^{3}H]WIN 35,428 and [^{3}H]nisoxetine, respectively (Table 1). The affinity of ZIENT and EIENT for the human DAT was 69 and 1.63-fold lower, respectively, than for SERT. In addition, the affinity of ZIENT and EIENT for the human NET was 474 and 20-fold lower, respectively, than for SERT. These results indicate that only ZIENT exhibited both high affinity and selectivity for human SERT vs both DAT and NET.

ZIENT was labeled with iodine-123, and the distribution of radioactivity expressed as percent dose per gram in selected tissues of male rats is shown in Table 2. The initial level of radioactivity in the entire brain after injection of [^{123}I]**6** was high. The brain uptake of [^{123}I]**6** exhibited a maximum at 5 min (0.83% dose/g) and exhibited a gradual washout from the brain over 2 h. After 2 h, the brain uptake (0.39% dose/g) had decreased 47% when compared to the uptake at 5 min. The accumulation of radioactivity in the thyroid was initially low and exhibited a gradual increase from 5 min (0.17% dose/organ) to 2 h (1.89% dose/g), which demonstrated the stability of the iodovinyl group to significant in vivo deiodination.

Table 2. Distribution of Radioactivity (% Injected Dose/g of Tissue) in Rat Tissues after iv Administration of [^{123}I]ZIENT

	percent injected, dose/g (range)			
region	time after injection: 5 min[a]	time after injection: 30 min[b]	time after injection: 60 min[b]	time after injection: 120 min[b]
blood	0.44 ± 0.05 (0.37−0.47)	0.40 ± 0.02 (0.37−0.42)	0.37 ± 0.05 (0.32−0.45)	0.31 ± 0.03 (0.28−0.34)
heart	0.81 ± 0.16 (0.71−1.04)	0.36 ± 0.02 (0.35−0.40)	0.29 ± 0.05 (0.21−0.36)	0.22 ± 0.05 (0.18−29)
lung	4.96 ± 0.59 (4.14−5.43)	1.59 ± 0.21 (1.24−1.78)	1.41 ± 0.41 (1.03−2.09)	0.76 ± 0.12 (0.60−0.88)
liver	0.38 ± 0.07 (0.31−0.45)	0.31 ± 0.06 (0.27−0.42)	0.22 ± 0.02 (0.21−0.24)	0.23 ± 0.11 (0.16−0.43)
spleen	1.81 ± 0.21 (1.55−2.04)	0.81 ± 0.08 (0.72−0.93)	0.61 ± 0.15 (0.44−0.85)	0.43 ± 0.06 (0.38−0.51)
kidney	1.13 ± 0.24 (0.86−1.45)	0.49 ± 0.03 (0.47−0.53)	0.34 ± 0.04 (0.29−0.38)	0.31 ± 0.05 (0.28−0.40)
muscle	0.23 ± 0.06 (0.19−0.33)	0.23 ± 0.01 (0.22−0.24)	0.20 ± 0.07 (0.17−0.23)	0.17 ± 0.03 (0.15−0.22)
testis	0.21 ± 0.02 (0.19−0.24)	0.34 ± 0.02 (0.32−0.37)	0.32 ± 0.02 (0.30−0.33)	0.31 ± 0.01 (0.29−0.32)
brain	0.83 ± 0.11 (0.69−0.97)	0.74 ± 0.04 (0.69−0.81)	0.62 ± 0.07 (0.53−0.71)	0.39 ± 0.07 (0.30−0.49)
thyroid	0.17 ± 0.02 (0.14−0.19)	0.49 ± 0.2 (0.27−0.78)	0.80 ± 0.25 (0.55−1.20)	1.87 ± 0.63 (1.15−2.87)

[a] Mean ± standard error and range values for four male Sprague−Dawley rats. [b] Mean ± standard error and range values for five male Sprague Dawley rats.

A regional distribution study in the brain of male Sprague−Dawley rats was performed with iodine-123 labeled ZIENT over 2 h. The results shown in Table 3 demonstrated that [^{123}I]**6** showed high initial hypothalamic uptake, a region rich in SERT sites, with excellent retention over time. The hypothalamus (Hyp) uptake reached a maximum at 60 min (0.77% dose/g). After 120 min, the hypothalamic uptake decreased 23% when compared to the peak activity at 60 min. The Hyp/Cereb ratio reached a maximum of 4.92 at 120 min. The prefrontal cortex (PFC), striatum (Str), and pons, brain regions also high in SERT sites, demonstrated good uptake and retention in comparison to the cerebellum (Cereb), a region with negligible SERT sites. The PFC/Cereb, Str/Cereb, and pons/Cereb ratios reached a maximum of 4.1, 4.0, and 3.3, respectively, at 120 min. The high uptake of iodine-123 in regions of the rat brain expressing SERT and the 23−33% washout in the Hyp, PFC, Str, and pons from 60 to 120 min demonstrate that [^{123}I]**6** has potentially favorable kinetic properties for in vivo quantitation and imaging of the SERT by SPECT.

To determine the in vivo selectivity of ZIENT for rat brain SERT, a series of blocking studies were performed in which unlabeled monoamine transporter specific blockers (2 mg/kg body weight) were administered intravenously 15 min prior to the intravenous administration of [^{123}I]ZIENT. The rats were sacrificed 60 min after injection of [^{123}I]ZIENT. The hypothalamus, striatum, prefrontal cortex, pons, and cerebellum were dissected, and the uptake of radioactivity was determined. The monoamine transporter blockers administered were fluvoxamine (SERT), RTI-113 (DAT), and

Table 3. Distribution of Radioactivity (% Injected Dose/g of Tissue) in Rat Brain Regions after iv Administration of [^{123}I]ZIENT

	percent injected, dose/g (range)			
region	time after injection: 5 min[a]	time after injection: 30 min[a]	time after injection: 60 min[b]	time after injection: 120 min[b]
hypothalamus (Hyp)	0.58 ± 0.05 (0.54−0.66)	0.76 ± 0.06 (0.69−0.78)	0.77 ± 0.07 (0.71−0.86)	0.59 ± 0.03 (0.56−0.63)
striatum (Str)	0.64 ± 0.08 (0.56−0.78)	0.72 ± 0.06 (0.72−0.81)	0.68 ± 0.15 (0.48−0.82)	0.49 ± 0.06 (0.41−0.54)
pons	0.59 ± 0.06 (0.51−0.66)	0.60 ± 0.06 (0.54−0.65)	0.59 ± 0.05 (0.54−0.64)	0.40 ± 0.05 (0.34−0.46)
prefrontal cortex (PFC)	0.77 ± 0.1 (0.66−0.82)	0.82 ± 0.13 (0.66−1.01)	0.82 ± 0.15 (0.64−1.00)	0.49 ± 0.07 (0.43−0.56)
cerebellum (Cereb)	0.53 ± 0.04 (0.48−0.57)	0.32 ± 0.03 (0.28−0.35)	0.25 ± 0.01 (0.24−0.27)	0.12 ± 0.01 (0.11−0.12)
Hyp/Cereb	1.09 ± 0.06	2.38 ± 0.08	3.08 ± 0.32	4.92 ± 0.3
Str/ Cereb	1.21 ± 0.09	2.25 ± 0.17	2.72 ± 0.59	4.0 ± 0.42
PFC/Cereb	1.45 ± 0.03	2.56 ± 0.04	3.28 ± 0.15	4.08 ± 0.7

[a] Mean ± standard error and range values for five male Sprague−Dawley rats. [b] Mean ± Standard error and range values for four male Sprague−Dawley rats.

Table 4. Distribution of Radioactivity (% Injected Dose/g of Tissue) in Rats 60 min after iv Administration of [^{123}I]ZIENT[a]

	study 1			study 2	
	no blocker[b,d]	fluvoxamine[b,d]	RTI-113[b,d]	no blocker[b]	reboxetine[c,d]
hypothalamus (Hyp)	0.92 ± 0.1[e,f] (0.83−1.06)	0.31 ± 0.02 (0.29−0.33)	0.80 ± 0.08[e,g] (0.70−0.89)	0.75 ± 0.13[f] (0.75−0.89)	0.65 ± 0.14[i] (0.5−0.76)
striatum (Str)	0.76 ± 0.15[e,f] (0.61−0.77)	0.30 ± 0.04 (0.27−0.35)	0.64 ± 0.09[e,g] (0.55−0.73)	0.63 ± 0.1[f] (0.52−0.72)	0.66 ± 0.04[i] (0.61−0.68)
prefrontal cortex (PFC)	0.93 ± 0.18[e,f] (0.74−1.16)	0.28 ± 0.03 (0.25−0.27)	0.78 ± 0.14[e,g,h] (0.67−0.98)	0.74 ± 0.22[f] (0.60−1.06)	0.69 ± 0.07[i] (0.61−0.72)
pons	0.62 ± 0.08[e,f] (0.57−0.74)	0.25 ± 0.03 (0.22−0.27)	0.56 ± 0.05[e,g] (0.53−0.61)	0.53 ± 0.13[f] (0.44−0.73)	0.54 ± 0.07[i] (0.46−0.60)
frontal cortex (FC)	0.75 ± 0.12[e,f] (0.68−0.93)	0.27 ± 0.03 (0.25−0.30)	0.66 ± 0.04[e,g] (0.63−0.71)	0.59 ± 0.08[f] (0.23−0.29)	0.63 ± 0.08[i] (0.55−0.71)
cerebellum (Cereb)	0.24 ± 0.03 (0.22−0.29)	0.17 ± 0.02 (0.16−0.19)	0.25 ± 0.02 (0.23−0.28)	0.19 ± 0.01 (0.18−0.20)	0.23 ± 0.04 (0.19−0.27)
Hyp/Cereb	3.83 ± 0.11	1.82 ± 0.16	3.20 ± 0.4	3.95 ± 0.57	2.83 ± 0.69
Str/Cereb	3.17 ± 0.26	1.76 ± 0.15	2.56 ± 0.43	3.32 ± 1.01	3.04 ± 0.59
Pfc/Cereb	3.88 ± 0.32	1.65 ± 0.09	3.12 ± 0.25	3.89 ± 1.35	3.07 ± 0.32
Pons/Cereb	2.58 ± 0.09	1.47 ± 0.07	2.24 ± 0.28	2.79 ± 0.58	2.35 ± 0.27

[a] Data analyzed via two way ANOVA with brain region and blocker as factors. *p* values were calculated using Tukey's test for all pairwise multiple comparisons. [b] Mean ± standard error and range values for four male Sprague−Dawley rats. [c] Mean ± standard error and range values for three male Sprague−Dawley rats. [d] Tissue studies performed with the same batch of [^{123}I]ZIENT. [e] $p < 0.001$ versus fluvoxamine. [f] $p < 0.001$ versus Cereb for no blocker. [g] $p < 0.001$ versus Cereb for RTI-113. [h] $p = 0.03$ versus PFC for no blocker. [i] $p < 0.001$ versus Cereb for reboxetine.

reboxetine (NET). The data (Table 4) from the rodent blocking studies were analyzed via a two-way ANOVA, and *p* values were calculated using Tukey's test for all pairwise multiple comparisons. (SigmaStat software package, SPSS, Inc., Chicago, IL). In the group of rats that received [^{123}I]ZIENT but no blocker, the uptake of radioactivity at 60 min postinjection in the hypothalamus, striatum, prefrontal cortex, pons, and frontal cortex was higher for each of these regions than in the cerebellum, a region with low levels of SERT protein ($p < 0.001$). This result is in agreement with the expected regional distribution of SERT protein in the rat brain. The same results were seen in the presence of the blockers RTI-113, a DAT selective ligand, and reboxetine, a NET selective ligand ($p < 0.001$). In contrast, administration of fluvoxamine, a SERT selective ligand, abolished the regional differences in uptake of activity, and the differences between uptake in the cerebellum and the other brain regions were not statistically significant. Together, these results indicate that the uptake of radioactivity in SERT-rich regions after administration of [^{123}I]ZIENT is due to binding to SERT sites. In addition, comparison of the no blocker groups with the RTI-113 and reboxetine groups showed no differences between the uptake of radioactivity in the brain regions studied with the exception of uptake in the prefrontal cortex, which was decreased in the RTI-113 group relative to the control group ($p = 0.03$). However, the lack of difference in uptake of activity between the no blocker and RTI-113 groups in the DAT-rich striatum indicates that significant binding of the radiotracer to the DAT did not occur.

Lipophilicity

Liophilicity has been shown to be an important property for achieving high initial brain uptake and subsequent specific binding of radioligands to brain regions rich in monoamine transporter and receptor binding sites. Several studies using the HPLC method of Brent et al.[27] involving a series of *N*-alkylspiperone analogues[28−30] have determined that initial brain uptake in rats and mice, as expressed by the percent injected per dose, is optimum when the measured log *P* values were 3.18−4.04. A recent study using an HPLC method[31] on a variety of lipophilic central nervous system (CNS) radioligands has determined that initial brain uptake of the radioligands is optimum when log $P_{7.4}$ = 2.4−2.8. Wilson et al. has also recently correlated biological activity in rats of a series of carbon-11 labeled 2-(phenylthio)araalkylamine[32] SERT ligands

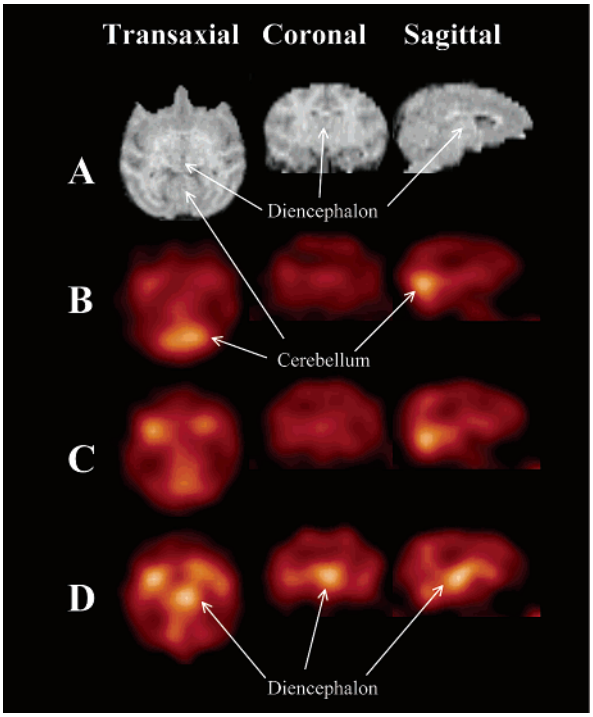

Figure 1. Transaxial, coronal, and sagittal images from SPECT acquisitions in a female cynomolgus monkey following administration of 6.5 mCi of [^{123}I]ZIENT (**6**). After reconstruction, the images were transformed to match an MRI brain image of the monkey (row A): SPECT images of [^{123}I]ZIENT at 42 min postinjection (row B); SPECT images of [^{123}I]ZIENT at 109 min postinjection (row C); SPECT images of [^{123}I]ZIENT at 239 min postinjection (row D).

to their lipophilicities. The measured log $P_{7.4}$ values using an octanol/water partition method at pH 7.4 ranged from 2.71 to 3.77. The lowest log $P_{7.4}$ value of 2.71 appeared to provide the best combination of initial brain uptake (1.22% dose/g) and specific to nonspecific binding ratios, 7.9−1, for SERT-rich midbrain regions to the cerebellum, respectively, at 60 min postinjection. The measured log $P_{7.4}$ value for ZIENT was 1.6 using the octanol/water partition method. This 1.6 value was below the optimum range. Nonetheless, [^{123}I]**6** achieved both acceptable brain penetrance (0.83% dose/g) at 5 min postinjection and specific (hypothalamus) to nonspecific binding (cerebellum) ratios (4.92−1) at 120 min postinjection.

In Vivo Nonhuman Primate Imaging

SPECT imaging studies in a cynomolgus monkey were performed using a dual-headed γ camera and [^{123}I]-**6** to determine time−activity curves for brain regions of interest at 10−239 min postinjection. The regional distribution of iodine-123 in the brain following administration of [^{123}I]**6** in this baseline scan was consistent with binding to SERT sites. The highest uptake in the cynomolgus monkey occurred in the diencephalon (Dien), a region encompassing the hypothalamus and thalamus and the striatum (Str). Uptake of radioactivity was also measured in the occipital cortex (Occx), whereas low uptake was detected in the frontal cortex (Fcx) and cerebellum (Cereb) (Figures 1 and 2).

Time−activity curves for the diencephalon, striatum, occipital cortex, frontal cortex, and cerebellum describing the kinetics of [^{123}I]**6** binding in the cynomolgus monkey are shown in Figure 2. Following administration of [^{123}I]**6**, the diencephalon and striatum exhibited the highest uptake and attained maximum uptake at 150−239 min. The diencephalon-to-cerebellum ratio was 1.33 at 58 min and increased to 1.85 at 239 min. The striatum-to-cerebellum ratio was 1.37 at 58 min and increased to 1.74 at 239 min. The occipital-cortex-to-cerebellum and frontal-cortex-to-cerebellum ratios were 1.2 and 1.04 at 239 min, respectively.

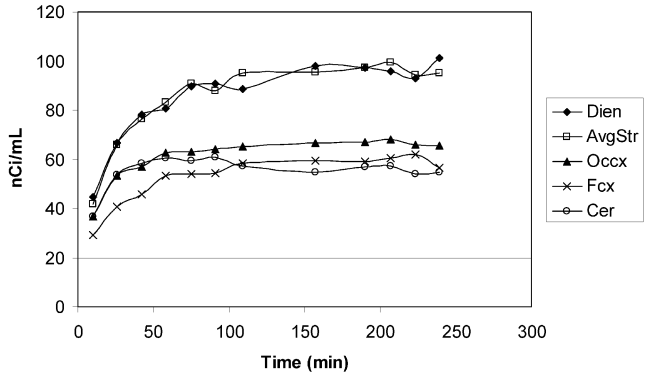

Figure 2. Time−activity curves for brain regions for a female cynomolgus monkey after receiving 6.5 mCi of [^{123}I]ZIENT (**6**). Serial images were acquired for a total time of 239 min.

An in vivo SPECT study of [^{123}I]**6** displacement by citalopram was performed in the same cynomolgus monkey to determine whether [^{123}I]**6** binding to diencephalon, striatum, occipital cortex, and frontal cortex reflected [^{123}I]**6** binding to SERT. A dose of citalopram (9 mg, 1.55 mg/kg body weight), a selective serotonin reuptake inhibitor, was administered intravenously and resulted in a significant reduction of the radioactivity in the diencephalon striatum, occipital cortex, and frontal cortex (Figures 3 and 4). The monkey was injected with [^{123}I]**6** 60 min prior to SPECT imaging, and time−activity curves for brain regions of interest at 70−190 min postinjection were determined for comparison with the baseline scan at 75−239 min. The highest uptake occurred in the diencephalon (Figure 3). The uptake of [^{123}I]**6** in diencephalon of the baseline scan from 75 to 239 min (Figure 2) was similar to its uptake in diencephalon from 70 to 190 min (Figure 4) in the chase scan prior to citalopram administration. The diencephalon attained maximum uptake at 162−190 min, whereas lower uptake was detected in the striatum, frontal cortex, and occipital cortex (Figure 4). The diencephalon-to-cerebellum ratio was 1.95 at 162 min, and the ratio increased to 2.12 at 190 min. The striatum-to-cerebellum ratio was 1.74 at 162 min and increased to 1.78 at 190 min. The frontal cortex-to-cerebellum and occipital-cortex-to-cerebellum ratios were 1.2 and 1.18 at 190 min, respectively. Following citalopram administration at 190 min postinjection, hypothalamus binding exhibited an average washout rate of 0.6%/min. One-hundred-one minutes after administration of citalopram, 39% of the [^{123}I]**6** radioactivity in the diencephalon and 31% of that in the striatum had been displaced. The 33% and 24% displacements of [^{123}I]**6** radioactivity in the occipital and frontal cortex, respectively, at 101 min after citalopram injection further indicate that [^{123}I]**6** binding reflects SERT labeling.

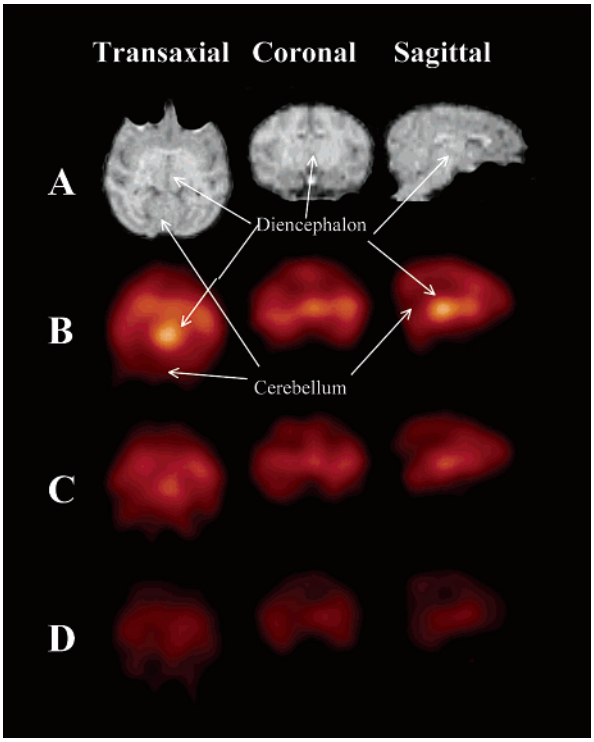

Figure 3. Transaxial, coronal, and sagittal images from SPECT acquisitions in a female cynomolgus monkey following administration of 7.5 mCi of [^{123}I]ZIENT (**6**) with citalopram administered at 190 min. After reconstruction, the images were transformed to match an MRI brain image of the monkey (row A): SPECT images of [^{123}I]ZIENT at 190 min postinjection (row B); SPECT images of [^{123}I]ZIENT at 233 and 43 min postinjection of citalopram (row C); SPECT images of [^{123}I]-ZIENT at 291 and 101 min postinjection of citalopram (row D).

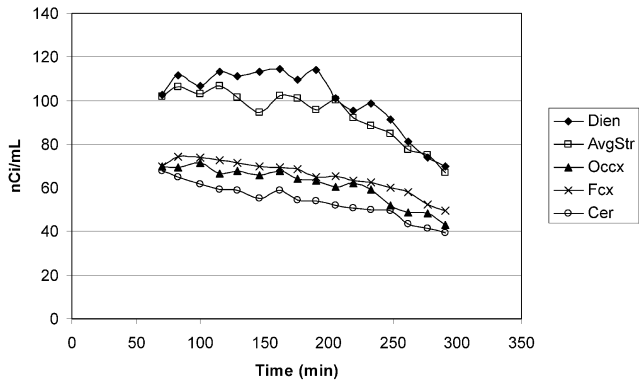

Figure 4. Time−activity curves for brain regions for a female cynomolgus monkey after receiving 7.5 mCi of [^{123}I]ZIENT (**6**) with citalopram administered at 190 min. Serial images were acquired for a total time of 291 min.

A SPECT imaging study in a rhesus monkey with the less potent and selective isomer, iodine-123 labeled EIENT, [^{123}I]**10**, was also performed. The in vivo specific binding of [^{123}I]**10** to the SERT and DAT-rich brain regions did not reflect its in vitro affinity, as reflected in poor-quality images (data not shown).

Arterial plasma samples from the cynomolgus monkey during the baseline scan taken following femoral vein injection of [^{123}I]ZIENT were analyzed for nonpolar, potentially brain permeable metabolites by a solvent extraction and HPLC method.[33] A radioactive component appearing in the initial arterial plasma samples was ether-extractable, displayed a major peak (> 96% pure) on HPLC spectra, and corresponded to the unmetabolized authentic [^{123}I]ZIENT. The fraction of plasma radioactivity corresponding to unmetabolized [^{123}I]ZIENT rapidly decreased from 26% at 15 min to 7.6% (93% pure) at 60 min. After 180 min, the fraction of plasma radioactivity corresponding to unmetabolized [^{123}I]ZIENT further decreased to 2.6% (93% pure). Analysis of monkey arterial plasma samples using HPLC separation and γ-counter detection showed the rapid appearance of one major polar (non-ether-extractable) metabolite of [^{123}I]ZIENT. The abundance of the polar metabolite as a percent of total plasma activity increased from 74% at 15 min to 97.4% at 180 min postinjection. The identity of the polar metabolite was not elucidated because of its improbable brain permeability. Thus, there was no detectable formation of lipophilic radiolabeled metabolites capable of entering the brain. The absence of labeled lipophilic metabolites in the arterial plasma that could reenter the brain permits the metabolism-uncorrected calculation of the [^{123}I]ZIENT input function and subsequent quantification of binding sites by tracer kinetic modeling without correcting for lipophilic metabolites.

Conclusions

Synthetic methods have been developed for the preparation of 2β-carbomethoxy-3β-(4′-((*Z*)-2-iodoethenyl)phenyl)nortropane (ZIENT) and 2β-carbomethoxy-3β-(4′-((*E*)-2-iodoethenyl)phenyl)nortropane (EIENT). Competition binding assays in cells stably expressing the human monoamine transporters demonstrated that ZIENT and EIENT have a high affinity for the SERT with ZIENT showing the higher selectivity. Biodistribution studies in rats showed that [^{123}I]ZIENT exhibited high specific uptake in the diencephalon, brainstem, and striatum, regions rich in SERT sites. In vivo SPECT imaging studies in monkeys demonstrated that pronounced uptake of [^{123}I]ZIENT occurred in the diencephalon with a transient equilibrium attained in less than 157 min and a rapid clearance from the cerebellum. These results support the candidacy of [^{123}I]ZIENT as a radioligand for in vivo quantitation of SERT sites by SPECT.

Experimental Section

All chemicals and solvents were analytical grade and used without purification. Sodium iodide containing iodine-123 was obtained from Nordion (British Columbia, Canada). The melting points (mp) were determined in capillary tubes using an electrothermal apparatus and are uncorrected. The thin layer chromatographic analyses (TLC) were performed using 250 μm thick layers of silica gel G PF-254 coated on aluminum plates (Whatman). The proton nuclear magnetic resonance (NMR) spectra were obtained at 300 or 400 MHz with a Varian instrument. Carbon-13 nuclear magnetic resonance spectra were obtained at 75 or 100 MHz with a Varian instrument. Elemental analyses were performed by Atlantic Microlab, Inc. (Norcross, Georgia) and, unless noted otherwise, were within $\pm$0.4% of the calculated values. High-resolution voltage scans were performed at 70 eV with reference scans over a narrow mass, 0.0006. Analyses were within 0.002 of theoretical values. Mass spectra (MS) were determined on a JEOL JMS-SX102/SX102A/E consisting of two SX102 double-focusing instruments followed by a JEOL HX110 ESA, using electronic ionization (EI) or fast atom bombardment (FAB).

All animal experiments were carried out according to protocols approved by the Institutional Animal Care and Use

Committee (IACUC) and Radiation Safety Committees of Emory University.

Chemistry. 2β-Carbomethoxy-3β-(4′-ethenylphenyl)-nortropane (2). Tributylvinyltin (423 μL, 1.4 mmol) and tetrakis(triphenylphosphine)palladium(0) (139 mg, 0.12 mmol) were added to a solution of 2β-carbomethoxy-3β-(4-bromophenyl)nortropane[26] (391 mg, 1.2 mmol) in 8 mL of toluene under argon. The resulting mixture was stirred, heated to gentle reflux for 8 h, and then cooled to room temperature. The solvents were removed under reduced pressure, and the residue was dissolved with 20 mL of Et_2O and filtered. The resulting filtered solid was washed with ether (2 × 15 mL). The combined filtrates were extracted with 3 N HCl (3 × 20 mL). The aqueous extracts were made basic with NH_4OH, extracted with CH_2Cl_2 (2 × 30 mL), dried over anhydrous $MgSO_4$, and concentrated in vacuo to yield the crude product[26] as a colorless oil (326 mg). The crude product was used in next step without purification. ^{1}H NMR ($CDCl_3$, 300 MHz): δ 7.34 (d, J = 8.4 Hz, 2H), 7.14 (d, J = 8.4 Hz, 2H), 6.67 (dd, J = 17.4, 10.8 Hz, 1H), 5.72 (d, J = 17.7 Hz, 1H), 5.22 (d, J = 10.8 Hz, 1H), 4.69 (br, 1H), 3.9−3.82 (m, 2H), 3.39 (s, 3H), 3.31−3.23 (m, 1H), 2.79−2.78 (m, 1H), 2.53−2.43 (m, 1H), 2.31−2.15 (m, 2H), 1.87−1.66 (m, 3H).

***N*-(*tert*-Butoxycarbonyl)-2β-carbomethoxy-3β-(4′-ethenylphenyl)nortropane (3).** A solution of di-*tert*-butyl dicarbonate (315 mg, 1.44 mmol) in 2 mL of CH_2Cl_2 was added to a stirred solution of **2** (326 mg, crude) in 5 mL of CH_2Cl_2 at 0 °C. The mixture was stirred at room temperature for 2 h. After the reaction, the solvents were removed and the residue was purified by flash column chromatography (hexane/ether, 3:1). The product **3** was isolated as a colorless oil (246 mg, 55% from **1**). ^{1}H NMR ($CDCl_3$, 300 MHz): δ 7.33−7.21 (m, 4H), 6.66 (dd, J = 17.7, 10.8 Hz, 1H), 5.69 (d, J = 17.7 Hz, 1H), 5.19 (d, J = 10.8 Hz, 1H), 4.68−4.43 (m, 2H), 3.45 (s, 3H), 3.28−3.21 (m, 1H), 2.90−2.74 (m, 2H), 2.18−1.64 (m, 5H), 1.47 and 1.43 (s, 9H). HRMS (FAB) Calcd for $C_{22}H_{29}LiNO_4$: 378.2257. Found: 378.2263.

***N*-(*tert*-Butoxycarbonyl)-2β-carbomethoxy-3β-(4′-formylphenyl)nortropane (4).** To a mixture of **3** (246 mg, 0.66 mmol) in 15 mL of THF/H_2O, 1:1, containing 2 mg of OsO_4 was added, at room temperature, $NaIO_4$ (284 mg, 1.32 mmol) in portions over 20 min. The resulting mixture was stirred for 21 h and poured into a 5% $NaHCO_3$ solution. The mixture was extracted with CH_2Cl_2, dried over $MgSO_4$, and evaporated. Purification of the residue by flash column chromatography with hexane/ether, 2.5:1, as eluent gave the product **4** as a colorless oil (221 mg, 89%). ^{1}H NMR ($CDCl_3$, 300 MHz): δ 9.96 (s, 1H), 7.80 (d, J = 8.1 Hz, 2H), 7.41 (d, J = 7.5 Hz, 2H), 4.71−4.45 (m, 2H), 3.45 (s, 3H), 3.35−3.29 (m, 1H), 2.95−2.77 (m, 2H), 2.20−1.67 (m, 5H), 1.47 and 1.43 (s, 9H). HRMS (FAB) Calcd for $C_{21}H_{27}LiNO_5$: 380.2049. Found: 380.2037.

***N*-(*tert*-Butoxycarbonyl)-2β-carbomethoxy-3β-(4′-((*Z*)-2-iodoethenyl)phenyl)nortropane (5).** To a suspension of iodomethyltriphenylphosphonium iodide (628 mg, 1.18 mmol) in 7 mL of dry THF was added sodium bis(trimethylsilyl)amide (1.2 mL, 1 M in THF, 1.2 mmol). The resulting mixture was stirred at room temperature for 1 min. The reaction mixture was then cooled to −78 °C, and **4** (221 mg, 0.59 mmol) in 4 mL of THF was added dropwise. After addition, the reaction mixture was allowed to warm to room temperature and stirred for 30 min. The resulting mixture was then poured into 5% $NaHCO_3$ solution. The mixture was extracted with CH_2Cl_2, dried over $MgSO_4$, and evaporated. Purification of the residue by flash column chromatography (hexane/ether, 3:1) afforded the product **5** as a colorless oil (255 mg, 51%). ^{1}H NMR ($CDCl_3$, 300 MHz): δ 7.57 (d, J = 8.1 Hz, 2H), 7.28−7.20 (m, 3H), 6.50 (d, J = 8.7 Hz, 1H), 4.67−4.43 (m, 2H), 3.45 (s, 3H), 3.30−3.21 (m, 1H), 2.91−2.78 (m, 2H), 2.18−1.64 (m, 5H), 1.47 and 1.43 (s, 9H). HRMS (FAB) Calcd for $C_{22}H_{28}ILiNO_4$: 504.1223. Found: 504.1226.

2β-Carbomethoxy-3β-(4′-((*Z*)-2-iodoethenyl)phenyl)-nortropane (6). A solution of 1.4 mL of TFA in 7 mL of CH_2Cl_2 was added to **5** (255 mg, 0.51 mmol). The resulting mixture was stirred at room temperature for 40 min and poured into a 5% $NaHCO_3$ solution. The product was extracted with CH_2Cl_2, dried over $MgSO_4$, and evaporated. The residue was purified by flash column chromatography (hexane/ether, 3:1) to afford the product **6** as a colorless oil (180 mg, 88%). ^{1}H NMR ($CDCl_3$, 300 MHz): δ 7.57 (d, J = 8.1 Hz, 2H), 7.29 (d, J = 8.1 Hz, 1H), 7.19 (d, J = 8.4 Hz, 2H), 6.55 (d, J = 8.7 Hz, 1H), 4.00−3.89 (m, 2H), 3.39 (s, 3H), 3.34−3.27 (m, 1H), 2.84−2.81 (m, 1H), 2.59−2.24 (m, 3H), 1.87−1.74 (m, 3H). ^{13}C NMR (100 Hz, $CDCl_3$): δ 173.99, 142.82, 138.42, 135.05, 128.50 (2C), 127.29 (2C), 78.97, 56.49, 53.79, 51.35, 51.15, 35.80, 33.73, 29.27, 27.84. HRMS (EI) Calcd for $C_{17}H_{20}INO_2$: 397.0539. Found: 397.0528. HPLC: Waters Nova-Pak C_{18} column 3.9 mm × 150 mm; absorbance wavelength 254 nm; eluent A, 25% H_2O in MeOH + 0.1% NEt_3, 1 mL/min, t_R = 8.57 min; eluent B, 30% H_2O in CH_3CN + 0.1% NEt_3, 1 mL/min, t_R = 5.57 min.

2β-Carbomethoxy-3β-(4′-((*Z*)-2-(trimethylstannylethenyl)phenyl)nortropane (7). To a solution of 2β-carbomethoxy-3β-(4′-((*Z*)-2-iodoethenyl)phenyl)nortropane (27 mg, 0.068 mmol) in 1.5 mL of THF was added hexamethylditin (48 mg, 0.136 mmol) and tetrakis(triphenylphosphine)palladium(0) (7 mg, 0.007 mmol). The mixture was stirred at 60 °C overnight. The solvent was evaporated, and the residue was purified by preparative TLC (silica gel, 10% MeOH in CH_2Cl_2). A crude product (6 mg) was obtained and then purified by HPLC (Waters, silica, 25 mm × 100 mm, 30% 2-propanol in hexane containing 0.1% Et_3N, 6 mL/min) to give the pure product (3 mg, 10%). ^{1}H NMR ($CDCl_3$, 300 MHz): δ 7.53 (d, J = 8.8 Hz, 1H), 7.18 (d, J = 8.7 Hz, 2H), 7.14 (d, J = 8.7 Hz, 2H), 6.16 (d, J = 8.8 Hz, 1H), 3.75−3.68 (m, 2H), 3.37 (s, 3H), 3.29−3.21 (m, 1H), 2.77−2.74 (m, 1H), 2.48−2.38 (m, 1H), 2.19−1.60 (m, 6H), 0.07 (s, 9H). ^{13}C NMR (100 Hz, $CDCl_3$): δ 174.09, 147.14, 141.67, 139.52, 133.52, 127.37 (4C), 56.47, 53.82, 51.38, 51.30, 35.59, 33.75, 29.22, 27.76, −7.89. HRMS (EI) Calcd for $C_{20}H_{29}NO_2Sn$ (^{120}Sn): 435.1220. Found: 435.1219.

2β-Carbomethoxy-3β-(4′-((*E*)-2-tributylstannylethenyl)-phenyl)nortropane (9). Alkyne **8**[25] (25 mg, 0.09 mmol) was dissolved in 5 mL of toluene containing tributyltin hydride (50 μL, 0.18 mmol) and azobisisopropionitrile (5 mg), and the resulting mixture was refluxed for 3 h under an argon atmosphere. After cooling to room temperature, the crude mixture was purified by flash column chromatography (silica, CH_2Cl_2/MeOH/NEt_3, 99:5:0.1) to afford the product **9** as a colorless oil (20 mg, 40%). ^{1}H NMR ($CDCl_3$, 300 MHz) δ 7.35−7.06 (m, 5H), 6.16 (d, J = 13.8 Hz, 1H), 3.89−3.85 (m, 2H), 3.39 (s, 3H), 3.32−3.26 (m, 1H), 2.80−2.70 (m, 1H), 2.51−2.43 (m, 1H), 1.58−1.29 (m, 12H), 0.98−0.87 (m, 15H). HRMS (FAB) Calcd for $C_{29}H_{48}NO_2Sn$ (^{120}Sn): 562.2707. Found: 562.2689.

2β-Carbomethoxy-3β-(4′-((*E*)-2-iodoethenyl)phenyl)-nortropane (10). Stannyl ester **9** (25 mg, 0.05 mmol) was dissolved in 5 mL of CH_2Cl_2, and the resulting solution was cooled to 0−5 °C. Iodine (23 mg, 0.09 mmol) in 1 mL of CH_2Cl_2 was added dropwise, and the resulting mixture was stirred until a pink solution resulted. The CH_2Cl_2 solution was washed with 10% $NaHSO_3$, dried over $MgSO_4$, and evaporated in vacuo to yield an oil. The crude material was purified by flash chromatography (silica, CH_2Cl_2/MeOH/NEt_3, 99:5:0.1) to afford **10** as a colorless oil (20 mg, 100%). ^{1}H NMR ($CDCl_3$, 400 MHz): δ 7.38 (d, J = 14.8 Hz, 1H), 7.21 (d, J = 8.4 Hz, 2H), 7.15 (d, J = 8 Hz, 2H), 6.77 (d, J = 14.8 Hz, 1H), 3.74−3.69 (m, 2H), 3.37 (s, 3H), 3.24−3.18 (m, 1H), 2.74−2.73 (m, 1H), 2.44−2.37 (m, 1H), 2.13−1.60 (m, 6H). Anal. Calcd for $C_{17}H_{20}NO_2I$: C, 51.40; H, 5.07; N, 3.53. Found: C, 51.17; H, 5.55; N, 3.50. HRMS (FAB) Calcd for $C_{17}H_{21}INO_2$: 398.0630. Found: 398.0617. HPLC: Waters Nova-Pak C_{18} column 3.9 mm × 150 mm; absorbance wavelength, 254 nm; eluent A, 75% MeOH/25% H_2O + 0.1% NEt_3, 1 mL/min, t_R = 11.31 min; eluent B, 70% CH_3CN/30% H_2O + 0.1% NEt_3, 1 mL/min, t_R = 7.53 min.

Radiolabeling. [^{123}I]-2β-Carbomethoxy-3β-(4′-((*Z*)-2-iodoethenylphenyl))nortropane (**6**) and [^{123}I]-2β-carbomethoxy-3β-(4′-((*E*)-2-iodoethenyl)phenyl)nortropane (**10**) were prepared by the method reported previously for [^{123}I]RTI-55.[34] Iodination kits were formulated by dispensing 300 μL (100 μg) of the tin substrate **7** or **9** solution (1 mg/3 mL of EtOH) into 1 mL vials.

Aqueous hydrogen peroxide (50 μL, 3% w/v) was added to a septum-sealed vial containing compound **7** or **9** (100 μg) in 300 μL of EtOH, 50 μL of 0.4 N HCl, and [^{123}I]-sodium iodide (no carrier added, specific activity of 240 Ci/μmol). The reaction proceeded at ambient temperature for 30 min and was quenched with 50 μL of 10% sodium bisulfite. The reaction mixture was drawn into a 3 mL syringe containing 500 μL of saturated $NaHCO_3$. The contents of the syringe were mixed and passed through a Waters classic C-18 sep-pak, pretreated with 8.5 mL of MeOH followed by 10 mL of H_2O. The sep-pak was eluted with 10 mL of H_2O to remove residual unreacted [^{123}I]sodium iodide. The radioiodinated product was isolated by elution with 10 mL fractions of MeOH/H_2O/NEt_3, 80:20:0.1. The eluent solution was evaporated in vacuo, and the residue was redissolved in 500 μL of MeOH/H_2O/NEt_3, 80:20:0.1. The solution containing [^{123}I]ZIENT was injected onto a reverse-phase HPLC column (Waters, 8 mm × 200 mm, flow rate 3 mL/min, 80:20:0.1 MeOH/H_2O/NEt_3). The fractions (30 s) eluting at 11−12 min containing the [^{123}I]ZIENT product were collected and evaporated in vacuo. The solution containing [^{123}I]EIENT was injected onto a reverse-phase HPLC column (Waters, 8 mm × 200 mm, flow rate 3 mL/min, MeOH:H_2O:NEt_3, 85:15:0.1). The fractions (30 s) eluting at 11−12 min containing the [^{123}I]EIENT product were collected and evaporated in vacuo. The radioiodinated products [^{123}I]-**6** and [^{123}I]-**10** were analyzed by HPLC (Waters C_{18}, 3.9 mm × 150 mm Novapak, MeOH/H_2O/NEt_3, 85:15:0.1%, flow rate 1 mL/min). The retention time (t_R) for [^{123}I]ZIENT and [^{123}I]EIENT was t_R = 6.9 min and t_R = 6.0 min, respectively. A UV detector and a radioactivity detector showed [^{123}I]ZIENT and [^{123}I]-EIENT to have a radiochemical purity and a specific activity of greater than 99% and 2 Ci/μmol, respectively. The specific activity measured was based on the detection limits of the UV detector. Fractions containing the greatest radioactivity were concentrated in vacuo, dissolved in sterile saline with 10% ethanol, and filtered through an Acrodisc 0.2 μm filter for in vivo studies. The radiochemical yield (decay-corrected to end of bombardment (EOB)) for [^{123}I]ZIENT and [^{123}I]EIENT was 45% (n = 5) and 42% (n = 4), respectively.

Lipophilicity Measurements. The measurement of log P of ZIENT between n-octanol and 0.02 M phosphate buffer at pH 7.4 was determined according to a previously published method.[32]

In Vitro Binding Experiments. Monoamine transporter binding assays used cell membranes from either a dog kidney (MDCK) cell line stably transfected with the human DAT cDNA (gift of Dr. Gary Rudnick, Yale University) or a human embryonic kidney cell line (HEK-293) stably transfected with either the human serotonin (hSERT) or norepinephrine transporter (hNET) cDNA (gift of Randy Blakely, Ph. D., Vanderbilt University). Cells were grown to confluency in DMEM containing 10% fetal bovine serum and geneticin sulfate and harvested using 37 °C phosphate-buffered saline (PBS, pH 7.4) containing ethylenediaminetetraacetic acid (EDTA). After centrifugation (2000g, 10 min), the supernatants were decanted and the pellets were homogenized with a Polytron PT3000 (Brinkman, Littau, Switzerland, 11,000 rpm for 12 s) in 30 volumes of PBS and centrifuged at 43000g for 10 min. The supernatants were decanted, and the resulting pellets were stored at −70 °C until assayed.

Binding assays were carried out in 12 mm × 75 mm polystyrene tubes in a 1000 μL volume consisting of 700 μL of assay buffer, 100 μL of competing ligand solution, 100 μL of ^{3}H ligand solution, and 100 μL of membrane suspension. Prior to each assay, the cell lines were characterized to determine a membrane concentration that yielded optimal binding. Membrane suspensions were prepared by resuspending the pellet in 5 mL of assay buffer and centrifuging (2000g, 10 min). The supernatant was decanted, and the resulting pellet was resuspended in assay buffer and briefly homogenized using a Polytron PT3000. Competing ligands were assayed in triplicate at each of 9−12 concentrations (10^{-13}−10^{-6} M). The ligands were first dissolved in absolute ethanol at 10^{-3} M and then serially diluted in 2.5 mM HCl. A monoamine transporter-selective ligand of known binding affinity (hDAT, GBR 12909; hSERT, fluvoxamine; hNET, desipramine) was included as a reference in each assay. For DAT binding, the assay buffer was 0.03 M phosphate buffer (pH 7.4) containing 0.32 M sucrose, the radioligand was [^{3}H]WIN 35,428 (Dupont NEN, Boston MA, 84.5 Ci/mmol, 2.0 nM final concentration), and the equilibrium incubation time was 2 h at 4 °C. For hSERT binding, the assay buffer was 50 mM Tris, 120 mM NaCl, 5 mM KCl (pH 7.9), the radioligand was [^{3}H]citalopram (Dupont NEN, Boston MA, 85.7 Ci/mmol, 0.5 nM final concentration), and the equilibrium incubation time was 1 h at 22 °C. For hNET binding, the assay buffer was 50 mM Tris, 300 mM NaCl, and 5 mM KCl (pH 7.4), the radioligand was [^{3}H]-nisoxetine (Dupont NEN, Boston MA, 85.9 Ci/mmol, 0.55 nM final concentration), and the incubation time was 4 h at 4 °C. All assays were initiated by the addition of membrane suspension. Incubations were terminated by the addition of 2 mL of 0.03 M phosphate buffer (pH 7.4, 4 °C) and rapid vacuum filtration through GF/B filters (presoaked in phosphate buffer containing 0.3% polyethyleneimine) with four washes (5 mL) of 0.03 M phosphate buffer (pH 7.4, 4 °C). The filters were then dried and placed in scintillation vials to which 6 mL of scintillation cocktail (Aquasol-2, Packard, Meriden, CT) was added. The vials were shaken and radioactivity determined in a liquid scintillation counter at 66% efficiency. The data from the competition binding curves were analyzed, and K_i values were generated using GraphPad Prism software (GraphPad Software, San Diego, CA).

Animal Tissue Distribution Experiments. The distribution of radioactivity was determined in tissues of male Sprague−Dawley rats (225−300 g) after intravenous administration of the radioiodinated tropanes. The animals were allowed food and water ad libitum prior to the experiment. The radioiodinated nortropane [^{123}I]**6** (10 μCi) in 0.2 mL of 10% EtOH in 0.9% NaCl was injected followed by a 0.4 mL of 0.9% NaCl flush directly into the tail vein of rats under ketamine anesthesia. The animals were sacrificed at various time points postinjection by cardiac excision under ketamine anesthesia, and the organs were excised, rinsed, and blotted dry. The organs were weighed, and the radioactivity of the contents was determined with a Packard automatic γ counter (model Cobra). The percent dose per gram of organ was calculated by a comparison of the tissue counts to suitably diluted aliquots of the injected material.

Regional brain distribution was obtained in male Sprague−Dawley rats (225−300 g) after intravenous administration of [^{123}I]**6**. The hypothalamus, prefrontal cortex, striatum, pons, and cerebellum were dissected and placed in tared test tubes. The test tubes were weighed, and the radioactivity of the contents was determined with a automatic γ counter. The percent injected dose per gram was calculated by a comparison of the decay-corrected tissue counts with the decay-corrected counts of the diluted initial injected dose. The uptake ratio of each brain region was obtained by dividing the percent injected dose per gram of each region by that of the cerebellum.

In Vivo Blocking Experiments. Male Sprague−Dawley rats (250−300 g) were allowed food and water ad libitum prior to the experiment and anesthetized as described above. [^{123}I]-ZIENT (10 μCi) in 0.2 mL of 10% ethanol in 0.9% NaCl was injected directly into the tail vein of the rats as described above. The animals were sacrificed at 60 min postinjection with an intramuscular injection of 0.2 mL/kg of euthanasia-5 (324 mg/50 mL, sodium pentobarbital) under anesthesia. One group was injected with RTI-113 (2 mg/kg) directly into the tail vein 15 min prior to the injection of [^{123}I]ZIENT. Another group of rats was injected intravenously with fluvoxamine (2 mg/kg) 15 min prior to injection of [^{123}I]ZIENT. A third group was injected with reboxetine (2 mg/kg), and a fourth group of rats was injected with [^{123}I]ZIENT only as the control group. The striatum, frontal cortex, prefrontal cortex, hypothalamus, pons, and cerebellum were dissected and placed in tared test tubes. The test tubes were weighed, and radioactivity was determined with a Packard automatic γ counter (model Cobra). The percent dose per gram was calculated by a comparison of

decay-corrected and background-subtracted tissue counts with the counts of the dilution-corrected initial injected dose.

Nonhuman Primate Imaging. Quantitative brain images were acquired in a female cynomolgus monkey weighing 5.8 kg. The monkey was fasted for 12 h. The animal was initially anesthetized with Telazol (3 mg/kg, im) and maintained on a 1% isofluorane/5% oxygen mixture throughout the imaging procedure. The animal was intubated with assurance of adequate patency of the airway and was placed on a ventilator with arterial blood gases monitored throughout the study to ensure physiologic levels of respiration. The female cynomolgus monkey's head was immobilized and positioned in an ADAC Vertex camera, and a bolus of radioligand ([^{123}I]**6**, 6.5 mCi) was injected iv over ~30 s. A dynamic SPECT sequence of scans (16 × 15 min) was obtained to measure regional brain uptake. SPECT images were reconstructed and registered with the monkey's MRI brain scan. Regions of interest were placed, using the MRI scan, over the diencephalon (thalamus and hypothalamus), striatum (caudate, putamen), frontal cortex, occipital cortex, and cerebellum. Time−activity curves were estimated by extracting maximal counts from each of the regions of interest for each of the SPECT acquisitions. In a second imaging session, the female cynomolgus monkey was again positioned in the ADAC Vertex camera as described above and a slow bolus of radioligand ([^{123}I]**6**, 7.5 mCi) was injected iv over ~30 s. A dynamic SPECT sequence (8 × 15 min) was obtained with the collection of emission data initiated at 90 min postinjection to measure regional brain uptake. SPECT images were reconstructed and registered with the monkey's MRI brain scan.The validation of [^{123}I]ZIENT binding to SERT in the diencephalons/brainstem, striatum, frontal cortex, and occipital cortex of the female cynomolgus monkey was obtained by its displacement by the potent SERT ligand citalopram. The dose of citalopram was 1.55 mg/kg of body weight administered 190 min following injection of [^{123}I]-ZIENT. Eight additional SPECT images were acquired and analyzed as described above.

[^{123}I]ZIENT Metabolite Analysis (Monkey). Arterial plasma analysis of [^{123}I]ZIENT metabolism was performed in one cynomolgus monkey. Metabolite analysis was performed as described for [^{18}F]FECNT.[33] [^{123}I]ZIENT was injected as described above, and arterial samples (5.0 mL) were collected at approximately 15, 30, 45, 60, 90, 120, 150, and 180 min after tracer injection. Plasma was prepared by centrifugation (3000*g* for 20 min), and nonpolar, brain-permeable ^{123}I-labeled metabolites were extracted with ethyl ether (2 × l mL). The ethyl ether extracts of each plasma sample were evaporated to dryness under nitrogen at 35 °C. The resulting residue was dissolved in 200 μL of MeOH/H_2O/NEt_3, 3:1:0.1%, and analyzed by HPLC with a UV detector (254 mm) and a flow-through radioactivity detector. Chromatographic separation used a Waters reverse-phase C_{18} column (8 mm × 200 mm) and a mobile phase of MeOH/H_2O/NEt_3 ,3:1:0.1%, and flow rate of 1 mL/min. Eluate fractions (0.4 min) were collected and measured for radioactivity using a Packard Cobra automatic γ counter.

Acknowledgment. This research was sponsored by the Office of Health and Environmental Research, U.S. Department of Energy, under Grant No. DE-FG02-97ER62637 and by the Emory Conte Center for the Neuroscience of Mental Disorders.

References

(1) Owens, M. J.; Nemeroff, C. B. The Serotonin Transporter and Depression. *Depression Anxiety* **1998**, *8* (Suppl. 1), 5−6.
(2) Perry, E. K.; Marshall, E. F.; Blesses, G.; Tomlinson, B. E.; Perry, R. H. Decreased Imipramine Binding in the Brains of Patients with Depressive Illness. *Br. J. Psychiatry* **1983**, *142*, 188−192.
(3) Stanley, M.; Virgilio, J.; Gershon, S. Tritiated [^{3}H]imipramine Binding Sites Are Decreased in the Frontal Cortex of Suicides. *Science* **1982**, *216*, 1337−1339.
(4) Leake, A.; Fairbairn, A. F.; McKeith, I. G.; Ferrier, I. N. Studies on the Serotonin Uptake Binding Site in Major Depressive Disorder and Control Post-Mortem Brain: Neurochemical and Clinical Correlates. *Psychiatry Res.* **1991**, *39*, 31−35.
(5) Owens, M. J.; Nemeroff, C. B. Role of Serotonin in the Pathophysiology of Depression: Focus on the Serotonin Transporter. *Clin. Chem.* **1994**, *40*, 288−295.
(6) Palmer, A. M.; Francis, P. T.; Benton, J. S.; et al. Presynaptic Serotonergic Dysfunction in Patients with Alzheimer's Disease. *J. Neurochem.* **1987**, *48*, 8−15.
(7) Cash, R.; Raisman, R.; Ploska, A. Y. High and Low Affinity [^{3}H]-Imipramine Binding Sites in Control and Parkinsonian Brain. *Eur. J. Pharmacol.* **1985**, *117*, 71−80.
(8) Chingaglia, G.; Landwehrmeyer, B.; Probst, A.; Palacios, J. M. Serotonergic Terminal Transporters Are Differentially Affected in Parkinson's Disease and Progressive Supranuclear Palsy: An Autoradiographic Study with [^{3}H]Citalopram. *Neuroscience* **1993**, *54*, 691−699.
(9) Squier, M. V.; Jalloh, S.; Hilton-Joneees, D.; Series, H. Death After Ectasy Ingestion: Neuropathological Findings. *J. Neurol., Neurosurg. Psychiatry* **1995**, *58*, 756.
(10) Ritz, M. C.; Lamb, R. J.; Goldberg, S. R.; Kuhar, M. J. Cocaine Receptors on Dopamine Tranporters Are Related to Self-Administration of Cocaine. *Science* **1987**, *237*, 1219−1223.
(11) Chumpradit, S.; Kung, M. P.; Panyachotipun, C.; Prapansiri, V.; Foulon, C.; Brooks, B. P.; Szabo, S. A.; Tejan-Buut, S.; Frazer, A.; Kung, H. F. Iodinated Tomoxetine Derivatives as Selective Ligands for Serotonin and Norepinephrine Uptake Sites. *J. Med. Chem.* **1994**, *37*, 1220−1223.
(12) Kung, M. P.; Chumpradit, S.; Billings, J.; Kung, H. F. 4-Iodtomoxetine: A novel ligand for serotonin uptake sites. *Life Sci.* **1992**, *51*, 95−106.
(13) Hashimoto, K.; Goromaru, T. High Affinity [^{3}H]6-Nitroquipazine Binding Sites in Rat Brain. *Eur. J. Pharmacol.* **1990**, *180*, 273−281.
(14) Hashimoto, K.; Goromaru, T. High Affinity Binding of [^{3}H]6-Nitroquipazine to Cortical Membranes in the Rat: Inhibition by 5-Hydroxytryptamine and 5-Hydroxytryptamine Uptake Inhibitors. *Neuropharmacology* **1991**, *30*, 113−117.
(15) Hashimoto, K.; Goromaru, T. In Vivo Labeling of 5-Hydroxytryptamine Uptake Sites in Mouse Brain with [^{3}H]6-Nitroquipazine. *J. Pharmacol. Exp. Ther.* **1990**, *255*, 146−153.
(16) Jagust, W. J.; Eberling, J. L.; Roberts, J. A.; Brennan, K. M.; Hanrahan, S. M.; Taylor, S.; VanBrocklin, H.; Enas, J. D.; Biegon, A.; Mathis, C. A. In Vivo Imaging of the 5-Hydroxytryptamine Reuptake Site in the Primate Brain Using Single Photon Computed Tomography and [^{123}I]-5-Iodo-6-nitroquipazine. *Eur. J. Pharmacol.* **1993**, *242*, 189−193.
(17) Jagust, W. J.; Eberling, J. L.; Biegon, A.; Taylor, S.; VanBrocklin, H.; Jordon, S.; Hanrahan, S. M.; Roberts, J. A.; Brennan, K. M.; Mathis, C. A. Iodine-123 5-Iodo-6-nitroquipazine: SPECT radiotracer to image the serotonin transporter. *J. Nucl. Med.* **1996**, *37*, 1207−1214.
(18) Oya, S.; Choi, S. R.; Hou, C.; Mu, M.; Kung, M.-P.; Acton, P. D.; Siciliano, M.; Kung, H. F. 2-((2-((Dimethylamino)methyl)-phenyl)thio)-5-iodophenylamine (ADAM): An Improved Serotonin Transporters Ligand. *Nucl. Med. Biol.* **2000**, *27*, 249−254.
(19) Choi, S. R.; Hou, C.; Oya, S.; Mu, M.; Kung, M.-P.; Siciliano, M.; Acton, P. D.; Kung, H. F. Selective in Vitro and in Vivo Binding of [^{125}I]ADAM to Serotonin Transporters in Rat Brain. *Synapse* **2000**, *38*, 403−412.
(20) Acton, P. D.; Choi, S. R.; Hou, C.; Plossl, K.; Kung, H. F. Quantification of Serotonin Transporters in the Non-human Primates Using [^{123}I]ADAM and SPECT. *J. Nucl. Med.* **2001**, *42*, 1556−1562.
(21) Boja, J. W.; Kuhar, M. J.; Kopajtic, T.; Yang, E.; Abraham, P.; Lewin, A. H.; Carroll, F. I. Secondary Amine Analogues of 3β-(4′-Substituted phenyl)tropane-2β-carboxylic Acid Esters and *N*-Norcocaine Exhibit Enhanced Affinity for Serotonin and Norepinephrine Transporters. *J. Med. Chem.* **1994**, *37*, 1220−1223.
(22) Fujita, M.; Takatoku, K.; Matoba, Y.; Nishiura, M.; Koayashi, K.; Inoue, O.; Nishimura, T. Differential Kinetics of [123I]beta-CIT Binding to Dopamine and Serotonin Transporters. *Eur. J. Nucl. Med.* **1996**, *23*, 431−436.
(23) Kuikka, J. T.; Tiihonen, J.; Bergstron, K. A.; Karhu, J.; Haartikainen, P.; Viinamaki, H.; Lansimies, E.; Lehtonen, J.; Hakola, P. Imaging of Serotonin and Dopamine Transporters in the Living Human Brain. *Eur. J. Nucl. Med.* **1995**, *222*, 3346−350.
(24) Booij, J.; Knol, R. J.; Reneman, L.; de Bruin, K.; Janssen, A. G. M.; Royen, E. A. Iodine-123 labelled nor-β-CIT binds to the serotonin transporter in vivo as assessed by biodistribution studies in rats. *Eur. J. Nucl. Med.* **1998**, *25*, 1666−1669.
(25) Davies, H. M.; Kuhn, L. A.; Thornley, C.; Matasi, J. J.; Sexton, T.; Childers, S. R. Synthesis of 3β-Aryl-8-azabicyclo[3.2.1]octanes with High Binding Affinities and Selectivities for the Serotonin Transporter Site. *J. Med. Chem.* **1996**, *39*, 2554−2558.
(26) Blough, B. E.; Abraham, P.; Mills, A. C.; Lewin, A. H.; Boja, J. W.; Scheffel, U.; Kuhar, M. J.; Carroll, F. I. 3β-(4-Ethyl-3-iodophenyl)nortropane-2β-carboxylic acid methyl ester as a high-affinity selective ligand for the serotonin transporter. *J. Med. Chem.* **1996**, *39*, 4027−4035.

(27) Brent, D. A.; Sabatka, J. A.; Minick, D. J.; Henry, D. W. A simplified high-pressure liquid chromatography method for determining lipophilicity for structure−activity relationships. *J. Med. Chem*. **1982**, *26*, 1014−1020.
(28) Moerlein, S. M.; Laufer, P.; Stocklin, G. Effect of lipophilicity on the in vivo localization of radiolabeled spiperone analogues. *Int. J. Nucl. Biol*. **1985**, *12*, 353−356.
(29) Coenen, H. H.; Laufer, P.; Stocklin, G.; Wienhard, K.; Pawlik, G.; Bocher-Schwarz, H. G.; Heiss, W. D. 3-*N*-(2-[^{18}F]Fluoroethyl)-spiperone: A novel ligand for cerebral dopamine receptor studies with PET. *Life Sci*. **1987**, *40*, 81−88.
(30) Welch, M. J.; Katzenellenbogen, J. A.; Mathias, C. J.; Brodack, J. W.; Carlson, K. E.; Chi, D. Y.; Dence, C. S.; Kilbourn, M. R.; Perlmutter, J. S.; Raichele, M. E.; Ter-Pogassian, M. M. *N*-(3-[^{18}F]Fluoroethyl)-spiperone: The preferred ^{18}F labeled spiperone analog for positron emission tomographic studies of the dopamine receptor. *Nucl. Med. Biol*. **1988**, *1*, 83−97.
(31) Kessler, R. M.; Ansari, M. S.; dePaulis, T.; Schmidt, D. E.; Clanton, J. A.; Smith, H. E.; Manning, R. G.; Gillespie, D.; Ebert, M. H. High affinity dopamine receptor D_2 radioligands 1. Regional rat brain distribution of iodinated benzamides. *J. Nucl. Med*. **1991**, *32*, 1593−1600.
(32) Wilson, A. A.; Ginovart, N.; Schmidt, M.; Meyer, J. H.; Threlkeld, P. G.; Houle, S. Novel radiotracers for imaging serotonin transporters by positron emission tomography: Synthesis, radiosynthesis, and in vitro and ex vivo evaluation of ^{11}C-labeled 2-(phenylthio)araalkylamines. *J. Med. Chem*. **2000**, *43*, 3103−3110.
(33) Goodman, M. M.; Shi, B.; Keil, R.; Martarello, L.; Xing, D.; Kilts, C. D.; Votaw, J.; Ely, T. D.; Deterding, T.; Lambert, P.; Owens, M. J.; Camp, V. M.; Hoffman, J. M. ^{18}F-Labeled FECNT: A selective dopamine transporter radioligand for PET. *Nucl. Med. Biol*. **2000**, *27*, 1−12.
(34) Zea-Ponce, Y.; Baldwin, R. M.; Laurelle, M.; Wang, S.; Neumeyer, J. L.; Innis, R. B. Simplified multidose preparation of iodine-123-β-CIT: A marker for dopamine transporters. *J. Nucl. Med*. **1995**, *36*, 525−529.

JM0100180